Synthetic properties of bright metal-poor variables. II. BL Her stars.

M. Di Criscienzo[1,2], F. Caputo[3], M. Marconi[1], S. Cassisi[4]

[1] **INAF-Osservatorio Astronomico di Capodimonte, Via Moiariello 16, 80131 Napoli, Italy;**

[2] **Università degli Studi di Roma "Tor Vergata", Via della Ricerca Scientifica 1, 00133, Roma, Italy;**

[3] **INAF-Osservatorio Astronomico di Roma, Via Frascati 33, 00040 Monte Porzio Catone, Italy;**

[4] **INAF-Osservatorio Astronomico di Collurania, Via Maggini, 64100 Teramo, Italy;**

Abstract. We investigate the properties of the so-called BL Her stars, i.e., Population II Cepheids with periods shorter than 8 days, using updated pulsation models and evolutionary tracks computed adopting a metal abundance in the range of Z=0.0001 to Z=0.004. We derive the predicted Period-Magnitude (PM) and Period-Wesenheit (PW) relations at the various photometric bands and we show that the slopes of these relations are in good agreement with the slopes determined by observed variables in Galactic globular clusters, independently of the adopted M_V(RR)-[Fe/H] relation to get the cluster RR Lyrae-based distance. Moreover, we show that also the distances provided by the predicted PM and PW relations for BL Her stars agree within the errors with the RR Lyrae based values. The use of the predicted relations with W Vir stars, which are Population II Cepheids with periods longer than 8 days, provides no clear evidence for or against a change in the PM and PW slopes around $P \sim 10$ days.

1. Introduction

Population II pulsating variables play a fundamental role in our understanding of the properties of old stellar populations as well as in the definition of the cosmic distance scale. Among them, RR Lyrae stars are definitively the most abundant and the ones currently used as tracers of dynamical and chemical properties. Moreover, they are used as standard candles to establish the globular cluster distance scale and they provide the calibration of secondary distance indicators such, e.g., the Globular Cluster Luminosity Function in external galaxies (see Di Criscienzo et al. 2005 and references therein).
However, other classes of radial pulsators are actually observed in globular clusters and similar metal-poor stellar fields. In the current nomenclature, they are named Population II Cepheids (P2Cs) and Anomalous Cepheids (ACs): the former ones, with periods P from ~ 1 to ~ 25 days, are observed in clusters with few RR Lyrae stars and blue Horizontal Branch (HB) morphology, while the latter, with $\sim 0.3 \leq P \leq \sim 2$ days, are observed in the majority of the Local Group dwarf galaxies which have been surveyed for variable stars. These two classes are both brighter but either less massive (P2Cs) or more massive (ACs) than RR Lyrae stars with similar metal content.
In three previous papers (Marconi, Fiorentino & Caputo

2004; Caputo et al. 2004; Fiorentino et al. 2006) dealing with the investigation of the ACs and their role as distance indicators, we discussed the pulsation and evolution properties of these variables and we showed that they originate from $Z \leq 0.0004$ central He-burning models more massive than $\sim 1.3 M_\odot$ which evolve through the pulsation region at luminosity and effective temperature which increase, on average, as the mass increases. Given the basic equation for radial pulsation ($P\rho^{1/2} = Q$, where ρ is the star density and Q is the pulsation constant), the effect of the higher luminosity is balanced by the larger mass and temperature and consequently, in spite of their bright luminosity, the ACs show periods that are not significantly longer than those typical of RR Lyrae stars.
Concerning the P2Cs, which are often separated[1] into BL Her stars ($\log P < 1$) and W Vir stars ($\log P > 1$), several authors (e.g., Gingold 1985; Bono, Caputo & Santolamazza 1997; Wallerstein & Cox 1984; Harris 1985; Wallerstein 1990, 2002) have already suggested that they originate from hot, low-mass stellar structures which started the main central He-burning phase in the blue side of the RR Lyrae gap and now evolve toward the

---

[1] In their recent reviev, Sandage & Tammann (2006) adopt a different classification. However, in the present paper we will use the classical one.

Asymptotic Giant Branch crossing the pulsation region with the luminosity and the effective temperature that increases and decreases, respectively, with decreasing the mass: for this reason, these bright low-mass pulsators should reach periods of several days. Moreover, as also shown by Caputo et al. 2004 (see their Fig. 4) on theoretical ground, at fixed period the ACs are more luminous than P2Cs, a feature which is at the origin of their supposed "anomaly".

On the observational side, Nemec, Nemec & Lutz (1994) derived metal dependent Period-Luminosity (PL) relations in various photometric bands, suggesting that observed P2Cs pulsate either in the fundamental and in the first-overtone mode and that the slopes of the PL relations are significantly different for the two modes. On the other hand, on the basis of a sample of P2Cs identified in the OGLE-II variable star catalogue for the Galactic bulge fields, Kubiack & Udalsky (2003) found that all the observed stars, which have periods from ~ 0.7 to about 10 days, follow the same PL relation. Similar results are derived by Pritzl et al. (2003) and Matsunaga et al. (2006) for P2Cs in Galactic globular clusters. Furthermore, these last two investigations support the hypothesis that the same PL relation holds for BL Her and W Vir stars, without a steepening of the slope for periods longer than $P \sim$ 10 days, as earlier suggested by McNamara (1995).

From the theoretical point of view, the pulsation models by Buchler & Moskalik (1992) and Buchler & Buchler (1994), as based on a linear and nonlinear radiative analysis, showed that the blue edge for first-overtone pulsation was very close (≤ 100 K) to the fundamental one, producing a very narrow region of FO-only pulsation. More recently, Bono, Caputo & Santolamazza (1997) computed nonlinear convective models, finding a good agreement between the predicted and the observed boundaries of the P2C instability strip and suggesting that the observed variables are pulsating in the fundamental mode with a typical mass of ~ 0.52-$0.59 M_{\odot}$.
However, the Bono, Caputo & Santolamazza (1997) nonlinear convective models, although able to provide reliable information also on the red edge of pulsation region, were limited to a quite restricted range of stellar parameters and adopted an old input physics (see Bono & Stellingwerf 1994 for details). For this reason, following our program dealing with a homogeneous study of radially pulsating stars with various chemical composition, mass and luminosity, in the present paper we discuss the results of updated pulsation models with mass 0.50-0.65$M_{\odot}$ and luminosity $\log L/L_{\odot}$ =1.81-2.41 in order to build a sound theoretical scenario for the analysis of the P2Cs. In particular, we will derive the predicted relations connecting evolutionary and pulsation properties for BL Her stars and we will verify their use as distance indicators.

The paper is organized as follows: in Section 2, we present the evolutionary and pulsation models, while in Section 3 we deal with the evolution-pulsation connection and we give the predicted relations. The comparison with

Table 1. Basic parameters of the pulsation models and resulting effective temperatures at the edges for fundamental and first-overtone pulsation (see Note). If no value is given at FOBE and FORE, we found only fundamental models. A helium abundance Y=0.24 and a mixing-length parameter l/H_p=1.5 has been adopted. Mass and luminosity are in solar units.

Z	M	$\log L$	FOBE[a]	FBE[b]	FORE[c]	FRE[d]
0.0001	0.60	1.95	-	6850	-	5750
		2.05	-	6750	-	5650
		2.15	-	6750	-	5550
	0.65	1.91	6950	6850	6050	5750
		2.01	6750	6850	6250	5750
		2.11	-	6750	-	5550
0.001	0.50	2.11	-	6650	-	5450
	0.50	2.41	-	6350	-	5150
	0.55	1.81	6850	6850	6350	5650
		1.91	-	6850	-	5550
		2.01	-	6750	-	5450
	0.65	1.81	7050	6750	6650	5750
		1.91	6850	6750	6150	5650
		2.01	6650	6850	6350	5650
0.004	0.55	1.81	-	6950	-	5750
		1.91	-	6850	-	5650
		2.01	-	6750	-	5450

Note: a) First Overtone Blue Edge; b) Fundamental Blue Edge; c) First Overtone Red Edge; d) Fundamental Red Edge.

observed variables is presented in Section 4 and the conclusion close the paper.

2. Theoretical framework

The pulsation models computed for the present paper, as listed in Table 1, adopt the same nonlinear, nonlocal and time-dependent convective hydrodynamical code and the same physical assumptions (i.e., equation of state and opacity tables) already used for the analysis of Classical Cepheids (Caputo et al. 2005; Marconi, Musella & Fiorentino 2005; Fiorentino et al. 2007), RR Lyrae stars (Marconi et al. 2003; Di Criscienzo et al. 2004) and Anomalous Cepheids (Marconi, Fiorentino & Caputo 2004; Fiorentino et al. 2006). In those papers, several relations connecting pulsational and evolutionary parameters were derived, whose slopes show a general consistency with the observed values. Moreover, they gave also a good agreement with the features of observed light curves of Classical Cepheids (Bono, Castellani & Marconi 2002) and RR Lyrae stars (Bono, Castellani & Marconi 2000; Castellani, Degl'Innocenti & Marconi 2002; Di Criscienzo, Marconi & Caputo 2004; Marconi & Clementini 2005). On this ground, our pulsation models appear in principle able to provide reliable information on the structural parameters of observed variables and, in turn, on the distance modulus, although we cannot exclude that the theoretical

results are affected by unknown systematic errors and that further work is need to refine our knowledge. However, we wish to emphasize that our computations provide a homogeneous pulsational scenario for the study of complex stellar systems where a variety of pulsating stars can be observed.

The model sequences discussed in the present paper are computed as one parameter families with constant chemical composition, mass and luminosity, by varying the effective temperature T_e by steps of 100 K. These models, which adopt a value of the mixing length parameter l/H_p=1.5 to close the system of convective and dynamic equations, are fully described by Marconi & Di Criscienzo (2007) and here we report only the results relevant for the purpose of the present paper. For the sake of the following discussion, let us firstly make clear that increasing (decreasing) by 100 K the effective temperature of the computed bluest (reddest) fundamental (F) or first-overtone (FO) model yields non-pulsating structures in the corresponding mode. Accordingly, we adopt the effective temperature of the computed bluest FO and F model, increased by 50 K, as the first-overtone (FOBE) and the fundamental blue edge (FBE) respectively, and the effective temperature of the reddest FO and F model, decreased by 50 K, as the first-overtone (FORE) and the fundamental red edge (FRE) respectively. This yields that the effective temperatures given in Table 1 have the intrinsic uncertainty of ± 50 K.

Starting with the models with $0.65M_\odot$ and $\log L/L_\odot$=1.81, we note that they follow the well known behaviour of RR Lyrae stars in that FO models are generally bluer than the F ones, but with the FORE redder than the FBE. As a consequence, we have that: *a)* the limits of the whole pulsation region are described by the FOBE and the FRE; *b)* both the pulsation modes are stable in the middle zone delimited by the FBE and the FORE; *c)* F-only pulsators are located between the FRE and the FORE and FO-only pulsators between the FBE and the FOBE. By increasing the luminosity, the whole pulsation region moves towards the red, but with a significant shrinking of the FO-only pulsation region. Based on the values listed in Table 1, the difference FOBE−FBE is ∼ +300 K at $\log L/L_\odot$=1.81 and ∼ +100 K at $\log L/L_\odot$=1.91. A further increase of the luminosity yields that the FOBE becomes redder than the FBE (with a difference FOBE−FBE ∼ −150 K at $\log L/L_\odot$=2.01), with the total disappearance of stable FO models at $\log L/L_\odot \geq 2.11$.

Varying the mass, we note that with $0.60M_\odot$ no FO model is stable at $\log L/L_\odot \geq 1.95$, while with $0.55M_\odot$ we get FOBE=FBE at $\log L/L_\odot$=1.80 and only F models above this luminosity level. On the other hand, by relying on the computations discussed by Marconi et al. (2003) and Di Crisdenzo et al. (2004), we recall that for models with $0.80M_\odot$ the difference FOBE−FBE is ∼ +400 K at $\log L/L_\odot$=1.72 and ∼ +200 K at $\log L/L_\odot$=1.91.

In summary, the results listed in Table 1 confirm earlier suggestions (see Tuggle & Iben 1972; Bono, Castellani

& Stellingwerf 1995; Bono, Caputo & Santolamazza 1997) that for each given mass and helium content there exists an "intersection" luminosity L_{IP} where FOBE=FBE, and that above this luminosity only the fundamental mode is stable. On this ground, one has that the red limit of the instability strip is always determined by the FRE, while the blue limit is given by the FOBE or the FBE depending on whether the luminosity is fainter or brighter, respectively, than L_{IP}.

Based on present computations and the quoted RR Lyrae models, we estimate at Y=0.24

$$\log L_{IP} \sim 2.3 + 1.9 \log M, \qquad (1)$$

where mass and luminosity are in solar units. Concerning the limits of the instability strip, we adopt

$$\log T_e(FOBE) = 3.970(\pm 0.004) - 0.057 \log L + 0.094 \log M, \qquad (2)$$

as determined by Marconi et al. (2003) from pulsation models with $L < L_{IP}$, while a linear interpolation through the present results gives

$$\log T_e(FBE) = 3.912(\pm 0.007) - 0.035 \log L + 0.048 \log M \qquad (3)$$

$$\log T_e(FRE) = 3.925(\pm 0.006) - 0.075 \log L + 0.118 \log M, \qquad (4)$$

where the uncertainties include the intrinsic uncertainty of ± 50 K on the FOBE, FBE and FRE temperatures. Moreover, we derive that the pulsation equation for the fundamental mode can be approximated as

$$\log P_F = 11.579(\pm 0.015) + 0.89 \log L - 0.89 \log M - 3.54 \log T_e \qquad (5)$$

while for the few first-overtone models we get $\log P_{FO} \sim \log P_F - 0.12$, at constant mass, luminosity and effective temperature.

Before proceeding, it is worth mentioning that the adopted helium content Y=0.24 accounts for the most recent estimate (Cassisi et al. 2003; Salaris et al. 2004) based on measurements of the R parameter[2] in a large sample of Galactic globular clusters. In any case, RR Lyrae models with Y=0.20 and 0.35 (Marconi, private communication) show that reasonable variations of the helium content ($\Delta Y = \pm 0.03$) in metal-poor stars have quite negligible effects on the effective temperature of the instability edges ($\Delta T_e \sim \pm 80$ K). Moreover, we wish to recall that the onset of pulsation depends also on the efficiency of convection in the star external layers, namely on the adopted value of the mixing length parameter l/H_p. Since the effect of convection is to quench pulsation and the depth of convection increases from high to low effective temperatures, we expect that varying the l/H_p value will modify the effective temperature at FRE by a larger amount with respect to FBE or FOBE. Indeed, the additional computations with l/H_p=2.0 computed by Marconi & Di Crisdenzo (2007) have confirmed the general trend

---

[2] This parameter is the number ratio of HB to Red Giant Branch stars brighter than the HB level
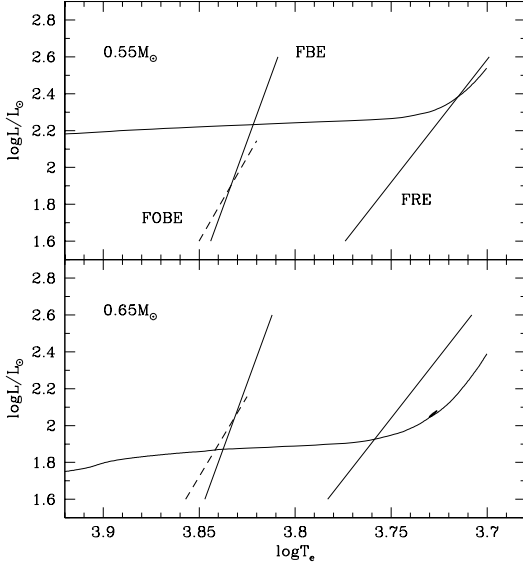
Fig. 1. Selected evolutionary tracks with Z=0.0001 and $[\alpha/\mathrm{Fe}]$=0.4 in comparison with the predicted FOBE, FBE and FRE. At luminosity levels brighter than the intersection between FOBE and FBE, we found only fundamental models.

shown by RR Lyrae (Marconi et al. 2003; Di Criscienzo et al. 2004) and Classical Cepheid models (Fiorentino et al. 2007) in that, at constant mass and luminosity, the FBE and FRE effective temperatures increase by ~ 100 and ~ 300 K, respectively. The effects of different l/H_p values on the predicted relations will be discussed in the following section.

Table 2. Chemical compositions of the adopted evolutionary models.

Z	Y	$[\alpha/\mathrm{Fe}]$	$[\mathrm{Fe/H}]$
0.0001	0.245	0.4	-2.62
0.001	0.246	0.4	-1.62
0.004	0.251	0.4	-1.01
0.0001	0.245	0.0	-2.27
0.001	0.246	0.0	-1.27
0.004	0.251	0.0	-0.66

For the evolutionary framework, we adopt the models computed by Pietrinferni et al. (2004, 2006) for scaled solar and α-enhanced ($[\alpha/\mathrm{Fe}]$=0.4) metal distributions in order to cover (see Table 2) the $[\mathrm{Fe/H}]$ range between -2.6 and -0.7. All the models have been transferred from the theoretical HR diagram to the various observational planes by adopting updated color-effective temperature relations and bolometric corrections (see Pietrinferni et al. 2004 and Cassisi et al. 2004) and the reader is referred to these papers[3] for information on the physical

---

[3] The whole set of stellar models can be retrieved at the following URL site: http://www.te.astro.it/BASTI/index.php.

Table 3. Luminosity L_{FBE} at the fundamental blue edge of the models with the labeled metal content and $[\alpha/\mathrm{Fe}]$=0.4, in comparison with the luminosity L_{IP} at the intersection between FOBE and FBE. The models in bold face are among those adopted for deriving the predicted relations (see text). The luminosity values are in solar units.

$M/M_\odot$	$\log L_{FOBE}$ Z=0.0001	$\log L_{FOBE}$ Z=0.001	$\log L_{FOBE}$ Z=0.004	$\log L_{IP}$
0.500	–	–	2.62	1.73
0.505	–	–	**2.39**	1.74
0.510	–	2.55	**2.28**	1.74
0.515	3.08	2.43	**2.20**	1.75
0.520	2.79	**2.32**	**2.15**	1.76
0.525	2.55	**2.25**	**2.08**	1.77
0.530	2.46	**2.21**	**2.02**	1.78
0.535	**2.38**	**2.16**	**1.99**	1.78
0.540	**2.32**	**2.11**	**1.94**	1.79
0.545	**2.27**	**2.07**	**1.89**	1.80
0.550	**2.24**	**2.04**	**1.83**	1.81
0.560	**2.16**	**1.98**	–	1.82
0.570	**2.10**	**1.95**	–	1.84
0.580	**2.05**	**1.88**	–	1.85
0.590	**2.02**	**1.87**	–	1.86
0.600	**2.01**	–	–	1.88
0.610	**1.96**	–	–	1.89
0.620	**1.93**	–	–	1.91

inputs and numerical assumptions. Here, it seems sufficient to note that this evolutionary framework is based on the most updated physical scenario and that the various stellar models have been followed all along the main core H-burning phase and advanced core and shell He-burning evolutionary phases. All the He-burning models adopted in present analysis have been computed by accounting for a He-core mass and He-envelope abundance on the Zero Age Horizontal Branch (ZAHB) characteristic on an Red Giant Branch (RGB) progenitor with initial total mass equal to $\sim 0.8 M_\odot$, corresponding to an age at the RGB tip of the order of 13 Gyr. The reliability and accuracy of the whole evolutionary scenario have already been tested by comparison with various empirical data sets (see also Riello et al. (2003); Salaris et al. (2004); Recio-Blanco et al. 2005) and, in summary, it appears quite suitable for investigating the populations of variable stars in Galactic globular clusters. Finally, let us note that these evolutionary computations represent, so far, the most updated and complete set of low-mass, He-burning models currently available. As a fact, the unique set of similar stellar models is the one published long time ago by Dorman, Rood & O'Connell (1993), which is based on physical inputs no more updated. However, in the following section we will discuss how the uncertainties in the evolutionary framework would affect the predicted relations.

The procedure for deriving the observational parameters of the predicted pulsators is in principle quite simple and has been described in several previous investigations
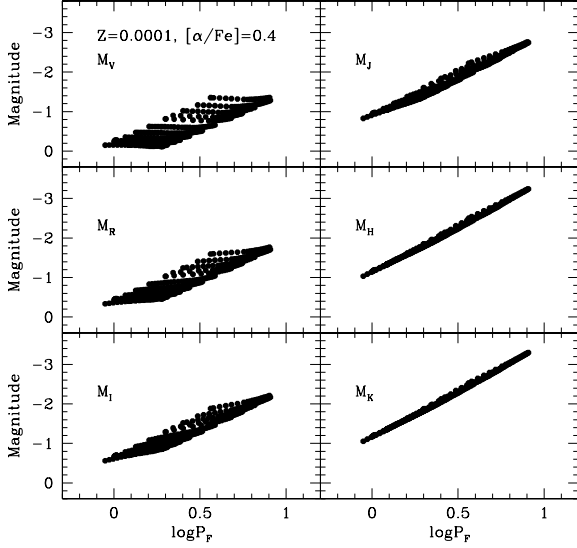
Fig. 2. Period-Magnitude diagrams of fundamental pulsators with l/H_p=1.5, Z=0.0001 and $[\alpha/\text{Fe}]$=0.4.

(Bono, Caputo & Santolamazza 1997; Marconi et al. 2003; Fiorentino et al. 2006). As shown in Fig. 1, the relations of the predicted edges of the instability strip [eqs. (2)-(4)] give us the way to select the models evolving with a luminosity larger than $\log L_{IP}$ and showing FBE$\geq \log T_e \geq$ FRE. In this way, we derive that the mass range of the predicted fundamental pulsators varies from 0.515-0.62$M_\odot$ at $[\text{Fe/H}]$=−2.6 to 0.50-0.55$M_\odot$ at $[\text{Fe/H}]$=−0.7. These mass values are in coherence with the mass range of the pulsating models listed in Table 1. However, as shown in Table 3, the average luminosity of the pulsators with a given mass increases as the metal content decreases, yielding that the $[\text{Fe/H}]$=−2.6 pulsators less massive than 0.53$M_\odot$ are more luminous than our brightest pulsating models. Since we cannot *a priori* be sure that the edge and period relations provided by the pulsation models listed in Table 1 can be extrapolated to higher luminosity levels, in the following we will use only the predicted pulsators whose mass and luminosity are consistent with those adopted for the pulsation models, as given in bold face in Table 3.

3. The connection between stellar evolution and pulsation

By calculating the fundamental period by means of Eq. (5) and adopting the magnitudes computed by Pietrinferni et al. (2004, 2006), we show in Fig. 2 selected Period-Magnitude (PM) diagrams of the predicted fundamental pulsators with l/H_p=1.5, Z=0.0001 and $[\alpha/\text{Fe}]$=0.4. Note that the resulting periods are in the range of about 0.8 to 8 days, making our theoretical investigations quite appropriate for the analysis of observed BL Her stars.

As already found for other pulsating variables, the effect of the intrinsic width in effective temperature of the instability strip (see Fig. 1) is greatly reduced when mov-

Table 4. Predicted PM_I, PM_J, PM_H and PM_K relations for fundamental pulsators with iron content in the range of $[\text{Fe/H}]$=−2.6 to −0.7 and $P \leq 8$ days.

$M_i = a + b\log P_F + c[\text{Fe/H}]+d(l/H_p - 1.5)$			
M_i	a	b	c	d
M_I	-0.26 ± 0.19	-2.10 ± 0.06	$+0.04\pm0.01$	-0.24
M_J	-0.64 ± 0.13	-2.29 ± 0.04	$+0.04\pm0.01$	-0.16
M_H	-0.95 ± 0.06	-2.34 ± 0.02	$+0.06\pm0.01$	-0.08
M_K	-0.97 ± 0.06	-2.38 ± 0.02	$+0.06\pm0.01$	-0.06
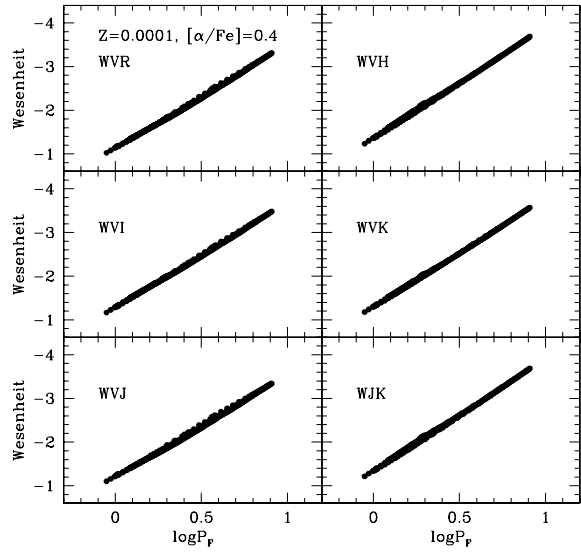
Fig. 3. Selected Period-Wesenheit diagrams of fundamental pulsators with l/H_p=1.5, Z=0.0001 and $[\alpha/\text{Fe}]$=0.4.

ing from optical to near-infrared magnitudes. On this basis, it is quite clear that synthetic PM_B to PM_R relations will significantly depend on the actual distribution of the pulsators within the pulsation region, at variance with the case of the near-infrared magnitudes. Moreover, we wish to recall that a variation of the mixing length parameter from l/H_p=1.5 to 2.0 gives hotter FBE and FRE by about 100 K and 300 K, respectively. Consequently, the pulsator distribution is slightly shifted toward shorter periods, yielding mildly steepened (less than 2%) and brighter PM relations, mainly in the optical bands. A least square fit to all the fundamental models yields the linear relations listed in Table 4: as a result, we get that the apparent distance modulus μ_I of observed variables can be determined within $\pm$ 0.20 mag, including the uncertainty due to the mixing-length parameter, whereas either μ_H and μ_K can be determined with a formal accuracy of 0.07 mag. Concerning the PM_J relation, given the residual effect of the intrinsic width of the instability strip, it yields μ_J within 0.15 mag.

It is widely acknowledged that the scatter in optical magnitudes can be removed if a Period-Magnitude-Color (PMC) is considered, i.e., if the pulsator magnitude is
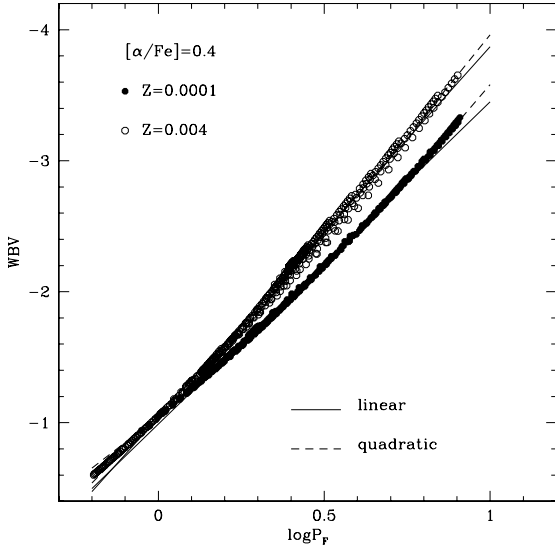
Fig. 4. WBV function versus period of selected fundamental pulsators with l/H_p=1.5. The solid and dashed lines are the linear and quadratic fit, respectively.

given as a function of the period and color. Several previous papers (see, e.g., Madore 1982; Madore & Freedman 1991; Tanvir 1999; Caputo et al. 2000, 2004) have already shown that the color coefficient of the various PMC relations is not too different from the extinction-to-reddening ratio provided by optical and near-infrared reddening laws (see Dean et al. 1978; Caldwell & Coulson 1987; Cardelli, Clayton & Mathis 1989; Laney & Stobie 1993). On this basis, the adoption of the reddening insensitive Wesenheit functions, where the magnitude is corrected for the color according to the interstellar extinction, removes also the largest part of the effect of differing effective temperatures. In the following, adopting $A_V = 3.1E(B-V)$, $A_R = 2.45E(B-V)$, $A_I = 1.85E(B-V)$, $A_J = 0.897E(B-V)$, $A_H = 0.574E(B-V)$ and $A_K = 0.372E(B-V)$, we will refer to the Wesenheit functions $WBV = V - 3.1E(B-V)$, $WVR = V - 4.77(V-R)$, $WVI = V - 2.48(V-I)$, $WVJ = V - 1.407(V-J)$, $WVH = V - 1.227(V-H)$ and $WVK = V - 1.136(V-K)$. Moreover, since only near-infrared data are available for several P2Cs, we will consider also the function $WJK=K - 0.709(J-K)$.

As shown in Fig. 3, where the fundamental pulsators with l/H_p=1.5, Z=0.0001 and [α/Fe]=0.4 are plotted is some selected Period-Wesenheit diagrams, the magnitude dispersion at fixed period is indeed greatly reduced, leading to tight linear PW relations. With regard to the effect of an increased value of the mixing length parameter, we find that moving from l/H_p=1.5 to 2.0 yields slightly brighter PW relations, while leaving almost unvaried (less than 2%) the slope. By a least square fit to all the fundamental pulsators, we derive the coefficients listed in Table 5. These relations give us a quite safe way to estimate the intrinsic distance modulus μ_0 of observed variables with a formal accuracy of ~ 0.1 mag, in-

Table 5. Period-Wesenheit relations for fundamental pulsators with iron content in the range of [Fe/H]=-2.6 to -0.7 and period $P \leq 8$ days.

$W = a + b\log P_F + c[\text{Fe/H}] + d(l/H_p - 1.5)$			
W	a	b	c	d
WVR	-1.07 ± 0.07	-2.42 ± 0.02	$+0.01\pm0.01$	-0.10
WVI	-1.16 ± 0.07	-2.43 ± 0.02	$+0.04\pm0.01$	-0.10
WVJ	-1.04 ± 0.06	-2.37 ± 0.02	$+0.05\pm0.01$	-0.08
WVH	-1.20 ± 0.06	-2.58 ± 0.02	$+0.06\pm0.01$	-0.07
WVK	-1.13 ± 0.06	-2.52 ± 0.02	$+0.06\pm0.01$	-0.06
WJK	-1.15 ± 0.06	-2.60 ± 0.02	$+0.06\pm0.01$	-0.06

dependently of the reddening. Concerning the WBV function, we show in Fig. 4 that the pulsator distribution in the $\log P_F$-WBV plane is much better represented by a quadratic relation, i.e., $WBV = \alpha + \beta\log P_F + \gamma(\log P_F)^2$, mainly at the lower metal content. Note also that, at variance with the other Wesenheit functions, the WBV function becomes brighter as the pulsator metal content increases, at fixed period, with the magnitude difference increasing towards the longer periods. As a whole, the least square fit to all the fundamental pulsators yields $\alpha = -1.06(\pm0.09)$, $\beta = -2.96(\pm0.08) - 0.36[\text{Fe/H}]$ and $\gamma = -0.17(\pm0.05) + 0.13[\text{Fe/H}]$.

In closure of this section, let us finally note that the dependence of the HB luminosity at the RR Lyrae gap on the metal content Z seems to be a robust result of stellar evolution and that all the available sets of evolutionary models, but few exceptions, predict similar trend (see Fig. 13 in Pietrinferni et al. 2004). Unfortunately, no comparison with other recent models can be made for He-burning low-mass models and for this reason we adopt an uncertainty of about ±0.04 dex of the logarithm luminosity as a safe estimate. However, when accounting for the dependence of the pulsation period on the stellar luminosity, this uncertainty on the stellar brightness *has no significative effects on the predicted PM and PW relations given in Table 4 and Table 5, respectively*. Indeed, an increase in the luminosity by 0.04 dex, for any fixed effective temperature, causes a period variation $\delta\log P$=0.036 while all the magnitudes and Wesenheit functions become brighter by 0.1 mag. As a consequence of these simultaneous variations, the "new" PM and PW relations will be brighter by 0.02 mag at most.

4. Comparison with observations

The Galactic globular clusters with observed P2Cs are listed in Table 6 with their reddening $E(B-V)$, apparent visual magnitude V(HB) and HB type, as given by Harris (1996). We recall that the HB type is the ratio (B$-$R)/(B+V+R), where V is the number of RR Lyrae variables, while B and R are the numbers of HB stars bluer and redder, respectively, than RR Lyrae stars. For all the P2Cs, we will adopt the periods and the apparent
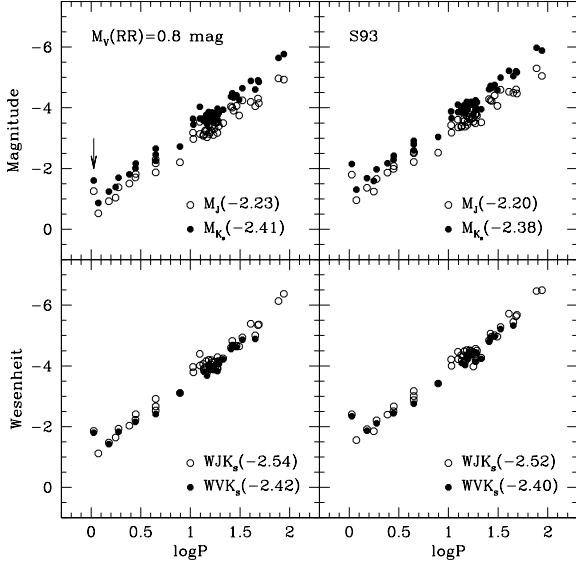
Fig. 5. PM and PW distributions of observed P2Cs under two different assumptions on the absolute magnitude of RR Lyrae stars. The numbers in parentheses are the slopes of the relations, as derived by a linear regression to the data. The arrow indicates V7 in NGC 6341. The infrared magnitudes are taken by Matsunaga et al. (2006).
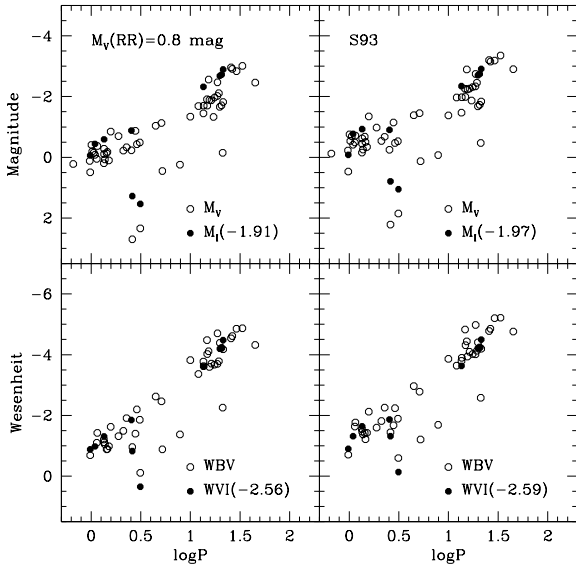
Fig. 6. PM and PW distributions of observed P2Cs under two different assumptions on the absolute magnitude of RR Lyrae stars. The outliers are V24 and V28 in NGC 4372, V12 and V32 in NGC 6205 and V3 in NGC 6254. The optical magnitudes are taken by Pritzl et al. (2003).

magnitudes provided by Pritzl et al. (2003, BVI, hereafter Pr03) and Matsunaga et al. (2006, JHK_s, hereafter Ma06).

In their investigations, Pr03 and Ma06 find quite tight linear correlations of the absolute magnitudes of P2Cs, as derived from RR Lyrae based distance mod-

uli, with $\log P$, without a clear evidence for a change in the slope between BL Her and W Vir stars. In particular, adopting $M_V(\mathrm{RR})=0.89+0.22[\mathrm{Fe/H}]$, Ma06 derive $\delta M_J/\delta\log P = -2.23(\pm0.05)$, $\delta M_H/\delta\log P = -2.34(\pm0.05)$ and $\delta M_{K_s}/\delta\log P = -2.41(\pm0.05)$, which are in excellent agreement with the predicted slopes given in Table 4. In that study, it is also mentioned that the slope of the observed near-infrared PM relations is not affected by different assumptions on the slope of the $M_V(\mathrm{RR})$-[Fe/H] relation. As a fact, by repeating the Ma06 procedure but adopting $M_V(\mathrm{RR})=0.8$ mag and $M_V(\mathrm{RR})=0.94+0.30[\mathrm{Fe/H}]$ (Sandage 1993: S93), we show in Fig. 5 (upper panels) that the variation to the near-infrared PM slopes is less than 2 percent. Here, we add that this holds also for the PW relations based on $VJHK_s$ magnitudes (lower panels). Note that the arrow in this figure refers to NGC 6341 V7 (Del Principe et al. 2005) which will be discussed separately.

Turning to the Pr03 optical magnitudes, some comments should be made to the data plotted in Fig. 6. Firstly, even removing the too faint outliers (i.e., the BVI data of V24 and V28 in NGC 4372 and the BV data of V12 and V32 in NGC 6205 and of V3 in NGC 6254, see also Pr03), we note a significant dispersion in the PM_V and $PWBV$ planes as well as some evidence that the W Vir stars follow steeper PM_V relations than the BL Her stars. As for the observed PM_I and $PWVI$ relations, they appear linear and quite tight, with the slope independent of the adopted $M_V(\mathrm{RR})$-[Fe/H] relation and in good agreement with the predicted values. However, it should be mentioned that these results are based on a rather small number of data points (mostly, the variables in NGC 6441).

In summary, we derive that all the observed P2Cs show linear near-infrared PM relations and linear PW relations, with the exclusion of WBV, independently of the adopted $M_V(\mathrm{RR})$-[Fe/H] relation. Moreover, the slopes of these relations are in close agreement with our predicted values for variables with $P \le 8$ days, supporting the hypothesis of similar relations for BL Her and W Vir stars. In addition, we wish to mention that the [Fe/H] effect on the zero-point of the near-infrared PM relations, as estimated by Ma06, is about 0.1 mag/dex^{-1}, again in agreement with our theoretical value.

On this ground, we can use the predicted relations derived in the previous section to derive the P2C distance moduli. With this purpose, since the Pietrinferni et al. (2004, 2006) magnitudes are in the Bessell & Brett (1988) near-infrared photometric system, the relations provided by Carpenter (2001) are used to transform the original 2MASS JHK_s data given by Ma06 into standard JHK magnitudes. For the P2C reddening and metal content, we adopt the values of the hosting globular cluster; however, for NGC 6388 and NGC 6441 we consider also [Fe/H]=-2.0, as adopted by Pr03 and Ma06.

By excluding the globular clusters with only W Vir stars and NGC 6341 V7, which will be discussed separately, we find some points worthy of mention:

– from the BVI magnitudes of the NGC 6441 P2Cs, we find an increasing discrepancy between the $\mu_{0,WBV}$ and $\mu_{0,WVI}$ values of a given variable when moving from short to long period stars. With [Fe/H]=−0.53, we get $\mu_{0,WBV} - \mu_{0,WVI} \sim 0.4$ mag at $\log P \sim 1.1$ and ~ 0.8 mag at $\log P \sim 1.3$. It is interesting to note that, if [Fe/H]=−2.0 is adopted, these differences are reduced to ~ 0 and ~ 0.3 mag, respectively. This would suggest that, despite the cluster high metallicity, the P2Cs may have a low metal content. However, we remind that the $\mu_{0,WBV}$ values are expected to be affected by large errors as a result of the older and less accurate photometry in these bands;

– for each given variable, the intrinsic distance modulus inferred by the near-infrared WJK function is in a general agreement with the values based on the WVJ, WVH and WVK functions. No sure comparison can unfortunately be made with $\mu_{0,WVI}$, whereas we note significant discrepancies with the results based on WBV. This can be due to some old BV data (see also Pr03), as well as, in the case of ω Cen variables, to the occurrence of a metallicity spread;

– except the variables in ω Cen, the trend of the intrinsic and the apparent distance moduli, as determined by JHK magnitudes, yields $A_J/E(B-V) \sim 0.85$, $A_H/E(B-V) \sim 0.54$ and $A_K/E(B-V) \sim 0.40$, in reasonable agreement with the extinction laws mentioned in Section 3.

Table 7. Mean intrinsic distance moduli (in magnitudes), as derived by the Wesenheit functions of BL Her and W Vir stars. The quantity N is the number of averaged values. As a matter of comparison, in the last column we give the intrinsic distance moduli based on RR Lyrae stars (see text).

name	μ_0(BLH)	N	μ_0(WV)	N	μ_0(RR)
N2808	14.99±0.06	1	–	–	14.90
N5139	13.84±0.08	4	13.78±0.16	4	13.62
N6254	13.39±0.20	4	13.56±0.16	2	13.23
N6273	14.69±0.06	1	14.77±0.06	2	14.71
N6284	15.77±0.06	2	–	–	15.93
N6293	14.80±0.06	1	–	–	14.76
N6402	14.80±0.08	8	14.93±0.09	8	14.86
N6441	15.55±0.07	2	15.53±0.19	6	15.28
N6441mp	15.61±0.07	2	15.58±0.18	6	15.60
N6715	17.19±0.10	2	–	–	17.16
N6749	14.56±0.08	1	–	–	14.51
N6779	15.05±0.06	4	15.31±0.11	4	15.08

Eventually, by excluding the $\mu_{0,WBV}$ values, we derive the mean intrinsic distance moduli listed in Table 7 together with the estimated total uncertainty. As a matter of comparison, we give in the last column the cluster distance determined by adopting the relation $M_V(\mathrm{RR})=0.89+0.22[\mathrm{Fe/H}]$ and the reddening and HB vi-

sual magnitude in Table 6. As a whole, given the well known debate on the RR Lyrae distance scale (see the recent review by Cacciari & Clementini 2003), we believe that the P2Cs distances agree with the RR Lyrae based values within the estimated uncertainty. As for a change in the PM and PW slopes around $\log P \sim 1$, namely between BL Her and W Vir stars, the values listed in Table 8 show similar distances for the variables in ω Cen and NGC 6441, whereas for the remaining clusters there is a subtle discrepancy as the former distance moduli are shorter by ~ 0.15 mag than the latter ones.

We can now study NGC 6341 V7 which has a period $\log P$=0.026 and is deviant from the near-infrared PM relations (see arrow in Fig. 5). With $VJHK$ data taken from Del Principe et al. (2005), we would derive μ_0=13.80±0.07 mag or 14.10±0.07 mag, depending on whether the variable is a fundamental or first-overtone BL Her star (i.e, adopting $\log P_F$=0.038). As a whole, these distances are too short with respect to $\mu_0(\mathrm{RR})$=14.65 mag, as derived by the relation $M_V(\mathrm{RR})$=0.89+0.22[Fe/H] using the values listed in Table 6. On the other hand, comparing the K magnitudes of RR Lyrae stars from Del Principe et al. (2005) with the predicted PM_K relations presented by Del Principe et al. (2006), we derive $\mu_0(\mathrm{RR})$=14.63±0.08 mag. Since the relations given in the present paper and those reported by Del Principe et al. (2006) are based on model computations which adopt homogeneous physics and numerical procedures, we can conclude that V7 is *not* a BL Her star but, due to the evidence that it is brighter than expected for its period, it may be an Anomalous Cepheid. Indeed, using for V7 the PM_K relations determined by Fiorentino et al. (2006) from evolutionary and pulsation models of fundamental ACs, we derive $\mu_K(\mathrm{AC})$=14.69±0.15 mag.

5. Conclusions

The main results of this study can be summarized as follows:

– On the basis of updated nonlinear convective pulsation models of BL Herculis we derive analytical relations for the boundaries of the instability strip as a function of the adopted stellar physical parameters, as well as the pulsation equation for these bright objects. Moreover, we confirm earlier suggestions that for each given mass and helium content there exists an "intersection" luminosity, as given by the intersection between the FOBE and the FBE, above which only the fundamental mode is stable.

– By combining the pulsational results with the predictions of the evolutionary models by Pietrinferni et al. (2004, 2006), we select models brighter than the "intersection" luminosity and therefore pulsating only in the fundamental mode, corresponding to periods longer than ~ 0.8d and stellar masses $\leq 0.62 M_\odot$.

– For the models which have masses and luminosities consistent with the physical parameters adopted in the

pulsation models, we derive the predicted PM and PW relations at the various photometric bands. We show that the predicted slopes are in close agreement with the empirical ones, quite independently of the slope in the adopted M_V(RR)-[Fe/H] relation.

– The predicted PM and PW relations have been applied to all the known P2Cs in Galactic globular clusters and the resulting distance moduli are in statistical agreement with the RR Lyrae based values.

– The variables in ω Cen and NGC 6441 seem to support the hypothesis of unique PM and PW relations for BL Her and W Vir stars. Conversely, for the remaining clusters the former distance moduli are found to be shorter by ~ 0.15 mag than the latter ones, suggesting steeper relations with $P \geq 10$ days. On this ground, no firm conclusion can presently be found in favor or against a change in the PM and PW slopes around $\log P \sim 1$.

– Finally, the application of the predicted relations to NGC6341 V7 provides evidence that this variable is not a P2C. Using the results presented by Fiorentino et al. (2006), we confirm the earlier suggestion by Ma06 that this star can be the second AC in Galactic globular clusters.

References

Bessell, M.S. & Brett, J.M., 1988, PASP, 100, 1134B
Bono, G., Castellani, V. & Marconi, M., 2000, ApJ, 532, L129
Bono, G., Castellani, V. & Marconi, M., 2002, ApJ, 565, L83
Bono, G., Caputo, F., Santolamazza, P., 1997, A&A, 317, 171
Bono, G., Castellani, V., & Stellingwerf, R.F., 1995, ApJ., 445, 145
Bono, G. & Stellingwerf, R.F., 1994, ApJS, 93, 233B
Buchler, J. R. & Moskalik, P., 1994, A&A, 292,450
Buchler,J. R. & Buchler, N. E. G.,1994,A&A,285, 213
Cacciari, C., & Clementini, G. 2003, in "Stellar Candles for the Extragalactic Distance Scale", Eds. D. Alloin and W. Gieren, Lecture Notes in Physics, 635, 105
Caldwell,J. A. R.& Coulson, I. M.,1987,AJ, 93, 1090
Cassisi, S., Salaris, M., Castelli, F., Pietrinferni, A., 2004,ApJ, 616, 498
Cassisi, S., Salaris, M. & Irwin, A. W., 2003, apJ, 588, 862
Castellani, V., Degl'Innocenti, S. & Marconi, 2002, A&A, 387, 861
Caputo, F., Marconi, M.; Musella, I.,2000, A&A, 354, 610
Caputo F., Bono, G., Fiorentino, G., Marconi, M., Musella, I., 2005, ApJ, 629, 1021
Caputo F., Castellani V., Degl'Innocenti S., Fiorentino G., Marconi M., 2004, A&A, 424, 927C
Cardelli, J.A., Clayton, G.C., & Mathis, J.S., 1989, ApJ, 345, 245C
Carpenter, J., 2001, AJ, 121, 2851
Cassisi, S., Salaris, M., Castelli, F. & Pietrinferni, A., 2004, ApJ, 616, 498
Dean, J. F.; Warren, P. R.; Cousins, A. W. J., 1978, MNRAS, 183, 569
Del Principe, M. et al., 2006, ApJ,(in press,astro-ph/0608052)
Del Principe, M.; Piersimoni, A. M.; Bono, G.; Di Paola, A.; Dolci, M.; Marconi, M., 2005, AJ,.129, 2714
Di Cris
cienzo, M., Marconi, M. & Caputo, F., 2004, ApJ, 612, 1092D
Di Crisienzo,M., Caputo, F., Marconi, M.,Musella, I.,2005, MNRAS, 365, 1357
Dorman, B., Rood., R. T. & O' Connel, R. W., 1993, 419,596
Fiorentino, G.,Limongi,M., Marconi, M., Caputo, F., 2006, A&A, (in press)
Gingold, R. A.,1985, MmSAI, 56, 169
Harris, H. C., 1985, AJ, 90, 756
Harris, H. C., 1996, AJ, 112, 1487
Kubiak, M. & Udalski, A., 2003, AcA, 53, 117
Laney, C. & Stobie, R. S., 1993,MNRAS,263,921L
Madore, B. F. 1982, ApJ, 253, 57
Madore, B. F., & Freedman, W. L. 1991, PASP, 103, 933
Marconi, M. & Di Crisienzo, M., 2007, A&A, in press (astro-ph/0701256)
Marconi, M., Caputo, F., Di Crisienzo, M., Castellani, M., 2003, ApJ, 596, 299M
Marconi, M., Fiorentino, G., & Caputo, F. 2004, A&A, 417, 1101
Marconi, M., Musella, I., & Fiorentino, G. 2005, ApJ, 632, 590
Matsunaga,N. et al., 2006, MNRAS, 370, 1979
McNamara, D. H., 1995, AJ, 109, 2134
Nemec, J.M., Nemec, A.F.L. & Lutz, T.E., 1994, AJ, 108, 222
Pritzl, B., Smith, H., Stetson, P., Catelan, M., Sweigart, A., Layden, A., Rich, R., 2003, AJ, 126, 1381
Pietrinferni, A, Cassisi, S., Salaris, M., & Castelli, F., 2006, ApJ, 642, 797

Pietrinferni, A, Cassisi, S., Salaris, M., & Castelli, F., 2004, ApJ, 612, 168

Recio-Blanco, A.; Piotto, G.; de Angeli, F.; Cassisi, S.; Riello, M.; Salaris, M.; Pietrinferni, A.; Zoccali, M.; Aparicio, A.2005, A&A, 432, 851R

Riello, M., Cassisi, S., Piotto, G., Recio-Blanco, A., De Angeli, F., Salaris, M., Pietrinferni, A., Bono, G., Zoccali, M.,2003, A&A, 410, 553

Sandage, A. & Tammann, G., 2006, ARA&A, 44. 93

Salaris, M., Riello, M., Cassisi, S., Piotto, G.,2004, A&A,420,911S

Sandage, A., 1993 ,AJ, 106, 687S

Stellingwerf, R.F., 1982, ApJ, 262, 330S

Tuggle, R. & Iben, I., 1972, ApJ, 8, 5

Wallerstein, G.,2002, PASP, 114, 689

Wallerstein, G. 1990, ASPC, 11, 56

Wallerstein, G.& Cox, A. N., 1984, PASP, 96, 677

Table 6. Galactic globular clusters with observed P2Cs listed with their reddening $E(B-V)$, iron content [Fe/H], apparent visual magnitude V(HB) and HB type, as given by Harris (1996). The last two columns give the numbers of BL Her and W Vir stars.

Name	$E(B-V)$	[Fe/H]	V(HB)	HB type	N_{BL}	N_{WV}
HP1	1.19	-1.55	18.60	$-$	0	2
N1904	0.01	-1.57	16.15	$+0.89$	0	1
N2419	0.11	-2.12	20.45	$+0.86$	1	0
N2808	0.22	-1.15	16.22	-0.49	1	0
N4372	0.39	-2.09	15.50	$+1.00$	2	0
N5139-ω Cen	0.12	-1.62	14.53	$+0.94$	9	2
N5272-M3	0.01	-1.57	15.68	$+0.08$	0	1
N5904-M5	0.03	-1.27	15.07	$+0.31$	0	2
N5986	0.28	-1.58	16.52	$+0.97$	0	1
N6093-M80	0.18	-1.75	16.10	$+0.93$	0	1
N6205-M13	0.02	-1.54	15.05	$+0.97$	4	1
N6218-M12	0.19	-1.48	14.60	$+0.97$	0	1
N6229	0.01	-1.43	18.03	$+0.24$	0	1
N6254-M10	0.28	-1.52	14.65	$+0.98$	1	2
N6256	1.03	-0.70	18.50	$-$	0	1
N6266-M62	0.47	-1.29	16.25	$+0.32$	0	1
N6273-M19	0.41	-1.68	16.50	$-$	1	2
N6284	0.28	-1.32	17.40	$-$	2	0
N6293	0.41	-1.92	16.50	$+0.90$	1	0
N6325	0.89	-1.17	17.90	$-$	0	2
N6341-M92	0.02	-2.28	15.10	$+0.91$	1	0
N6388	0.37	-0.60	16.85	$-$	2	1
N6402-M14	0.60	-1.39	17.30	$+0.65$	2	3
N6441	0.47	-0.53	17.51	$-$	2	5
N6453	0.66	-1.53	17.53	$-$	0	2
N6569	0.55	-0.86	17.52	$-$	0	1
N6626-M28	0.40	-1.45	15.55	$+0.90$	0	2
N6626-M28	0.40	-1.45	15.55	$+0.90$	0	1
N6715-M54	0.15	-1.58	18.17	$+0.75$	2	0
N6749	1.50	-1.60	19.70	$+1.00$	1	0
N6752	0.04	-1.56	13.70	$+1.00$	1	0
N6779-M56	0.20	-1.94	16.16	$+1.00$	1	1
N7078-M15	0.10	-2.26	15.83	$+0.67$	2	1
N7089-M2	0.06	-1.62	16.05	$+0.96$	0	4
Ton1	2.28	-1.30	21.40	$-$	0	1